ELSEVIER

Palaeogeography, Palaeoclimatology, Palaeoecology 202 (2003) 97–118

PALAEO

www.elsevier.com/locate/palaeo

Isotopic evidence for Late Jurassic–Early Cretaceous climate change

Darren R. Gröcke [a,b,*], Gregory D. Price [c], Alastair H. Ruffell [d], Jörg Mutterlose [e], Evgenij Baraboshkin [f]

[a] *Department of Geology, Royal Holloway University of London, Egham Hill, Egham, Surrey TW20 0EX, UK*
[b] *School of Geography and Geology, McMaster University, Hamilton, ON, Canada L8S 4K1*
[c] *Department of Geological Sciences, University of Plymouth, Drake Circus, Plymouth PL4 8AA, UK*
[d] *School of Geography, The Queen's University, Belfast BT7 1NN, Northern Ireland, UK*
[e] *Institut für Geologie, Mineralogie und Geophysik, Ruhr-Universität Bochum, Universitätsstraße 150, D-44801 Bochum, Germany*
[f] *Lomonosov State University, Geology Faculty, Department of Historical and Regional Geology, Vorobjovy Gory, Moscow 199899, Russia*

Received 18 January 2002; received in revised form 2 September 2003; accepted 5 September 2003

Abstract

Strontium-, oxygen- and carbon-isotope ratios have been determined from Late Jurassic–Early Cretaceous belemnites from the Volga Basin, Russia, and Kawhia Harbour, New Zealand. $^{87}Sr/^{86}Sr$ ratios derived from well-preserved belemnites from the Volga Basin support a Middle Tithonian age derived from the analysis of the endemic ammonite fauna. The Kawhia Harbour section records a gradual rise in $^{87}Sr/^{86}Sr$ values and in comparison with the published $^{87}Sr/^{86}Sr$ curve suggests that the lower part of the section is latest Oxfordian in age, whilst the upper part of the section correlates well with the biostratigraphic correlation suggestion of an Early–Middle Tithonian age. Although the published strontium calibration curve shows a degree of scatter, our new data confirm the uniform rise in $^{87}Sr/^{86}Sr$ values from the Late Jurassic into the Early Cretaceous. Such an increase may result from either a decrease in mid-oceanic ridge spreading and/or an increase in weathering rates and flux of radiogenic strontium, although a eustatic drop in sea level and concurrent Western Cordillera uplift suggests that weathering may have been the controlling factor of Late Jurassic seawater strontium-isotope composition. Palaeotemperatures derived from the well-preserved belemnite $\delta^{18}O_{carb}$ values from the Volga Basin indicate that the Middle Volgian (Late Kimmeridgian) was warm ($\sim$14–20°C), followed by a slight cooling and a subsequent gradual increase to the Jurassic–Cretaceous boundary. The $\delta^{18}O_{carb}$ values from New Zealand (located at a palaeolatitude of $\sim$80°S), if interpreted in terms of palaeotemperature, indicate a high degree of variability. Such variability may not be related to palaeotemperature, but to changes in oceanic chemistry resulting from the formation and dissolution of an ice-sheet and/or snow during the Oxfordian–Kimmeridgian. Carbon-isotope trends for the Late Jurassic show a fall in values from the Oxfordian with lowest values occurring in the Early–Middle Tithonian, before rising but without reaching values obtained in the Oxfordian. The overall low $\delta^{13}C_{carb}$ may be related to a global increase in continental weathering and/or upwelling of cooler oceanic water enriched in oxidised organic carbon (^{12}C-enriched).

* Corresponding author. Tel.: +1-905-525-9140; Fax: +1-905-546-0463.
E-mail address: d.grocke@mcmaster.ca (D.R. Gröcke).

0031-0182/03/$ – see front matter © 2003 Elsevier B.V. All rights reserved.
doi:10.1016/S0031-0182(03)00631-X

Keywords: seawater strontium; stable isotopes; palaeoclimate; ice-sheets; Late Jurassic; Early Cretaceous

1. Introduction

The Late Jurassic–Early Cretaceous was characterised in many areas of the world by a sea-level lowstand (Haq et al., 1987; Ziegler, 1990; Sahagian et al., 1996; Hardenbol et al., 1998; Hallam, 2001) possibly initiated by low spreading rates, resulting in large semi-restricted epicontinental seas and widespread deposition of non-marine sediments. Semi-restricted epicontinental seas during these times promoted provinciality particularly amongst molluscan faunas (e.g. Hallam, 1994). Current ideas concerning palaeotemperature and oceanic circulation patterns for the Late Jurassic and Early Cretaceous are contradictory.

Frakes (1979) and Hallam (1981, 1985) considered the Cretaceous to be a period of great warmth with tropical–subtropical conditions prevailing to at least 45°N and possibly to 70°S and warm to cool–temperate climates extending to the poles. Mean annual temperatures were significantly higher and latitudinal gradients only about half those of today (Frakes, 1979; Hallam, 1981). However, a number of studies postulate seasonally cold ocean temperatures and limited polar ice caps for the Early Cretaceous, though at least the presence of glaciers in places where seasonal (non-glacial) ice rafting occurs (e.g. Frakes and Francis, 1988; Frakes et al., 1992; Stoll and Schrag, 1996; Ditchfield, 1997; Price, 1999; Mutterlose and Kessels, 2000). The supposed global sea-level lowstand has also been taken as signifying the existence of short-lived glaciations with cool atmospheric conditions and a decrease in the rate of carbon cycling (Haq et al., 19887; Frakes et al., 1992; Weissert and Lini, 1991; Weissert and Mohr, 1996). Oxygen-isotope data from Europe suggest warm, temperate climates in the supposedly arid Late Jurassic (Bowen, 1961, 1966; Price and Sellwood, 1994; Anderson et al., 1994; Ditchfield, 1997; Podlaha et al., 1998; Riboulleau et al., 1998). A number of studies focusing particularly on Tethyan successions have assessed carbon-isotope variation during the Late Jurassic–Early Cretaceous (e.g. Weissert and Channell, 1989; Weis-

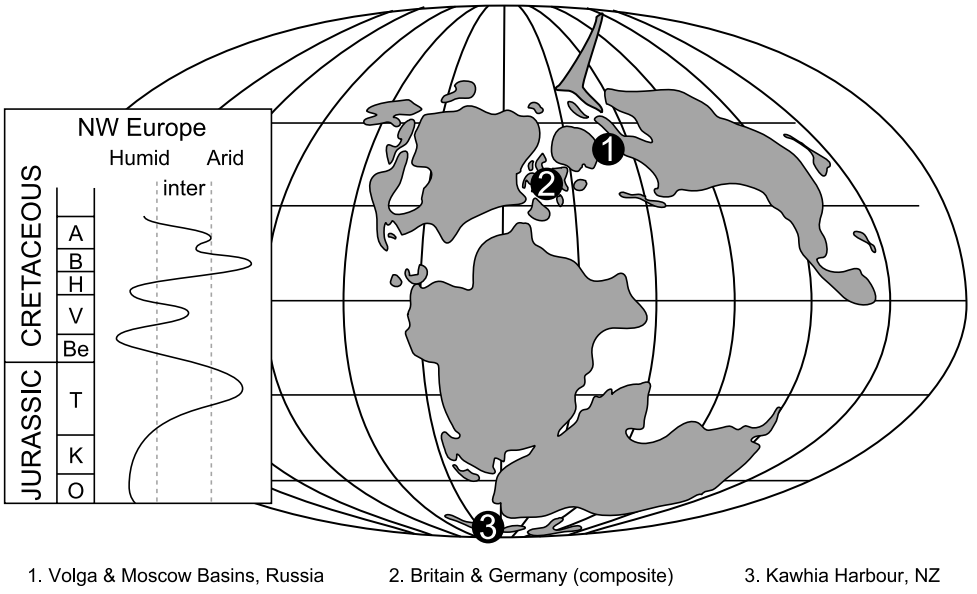

Fig. 1. Palaeogeographic reconstruction of the world during the Kimmeridgian showing investigated localities (based on Smith et al., 1994). Aridity–humidity curve for NW Europe (adapted from Price, 1999).

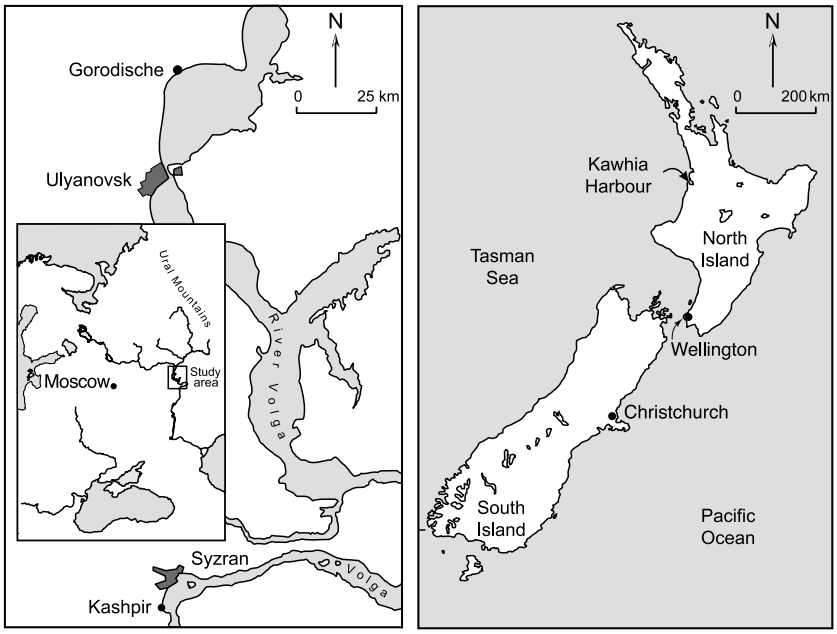

Fig. 2. Maps showing locations of Gorodische and Kashpir, Volga Basin, and Kawhia Harbour, New Zealand.

sert and Mohr, 1996; Bartolini et al., 1999). These studies document a number of minor positive carbon-isotope events overriding a generally stable curve, and relate them to episodes of increased weathering, nutrient availability and/or enhanced organic-carbon burial. These minor positive carbon-isotope events are surprising since the Kimmeridge Clay Formation (southern England) has sedimentary organic-carbon contents up to 35% (e.g. Blackstone Band) and other periods where major organic-carbon burial has taken place during the Early Jurassic and Cretaceous these are generally associated with positive carbon-isotope events (e.g. Jenkyns, 1999). The oxygen- and carbon-isotope analysis of belemnites has also been widely used as a quantitative means of investigating palaeoenvironmental variation. A major problem in isotopic studies of this kind has been the susceptibility of skeletal carbonates to diagenetic alteration resulting in a masking of the primary palaeoecological and/or palaeoceanographic signal (Marshall, 1992; Price et al., 1998). Scanning electron microscopy, cathodoluminescence, carbonate staining (following the methodology of Dickson, 1966) and trace-element analysis of the belemnites has been employed to help eliminate any trends originating from diagenetic overprinting (Elderfield, 1986; Brand and Morrison, 1987).

The strontium-isotope curve for the Late Jurassic–Early Cretaceous is relatively scattered, but indicates a general rise in $^{87}Sr/^{86}Sr$ during the Late Jurassic (Jones, 1992; Jones et al., 1994a; Podlaha, 1995; Podlaha et al., 1998; Gröcke, 2001; Price and Gröcke, 2002; Jenkyns et al., 2002). Hence, the aim of this study is to determine belemnite strontium-, carbon- and oxygen-isotope ratios during the Late Jurassic–Early Cretaceous interval from successions in the Volga Basin, SE Russia, and Kawhia Harbour, New Zealand (Fig. 1). $^{87}Sr/^{86}Sr$ values from belemnites provide an effective means to correlate the sections from Russia and New Zealand with the NW European ammonite zonal scheme.

2. Geological setting

2.1. Volga Basin, SE Russia

During the Late Jurassic–Early Cretaceous the

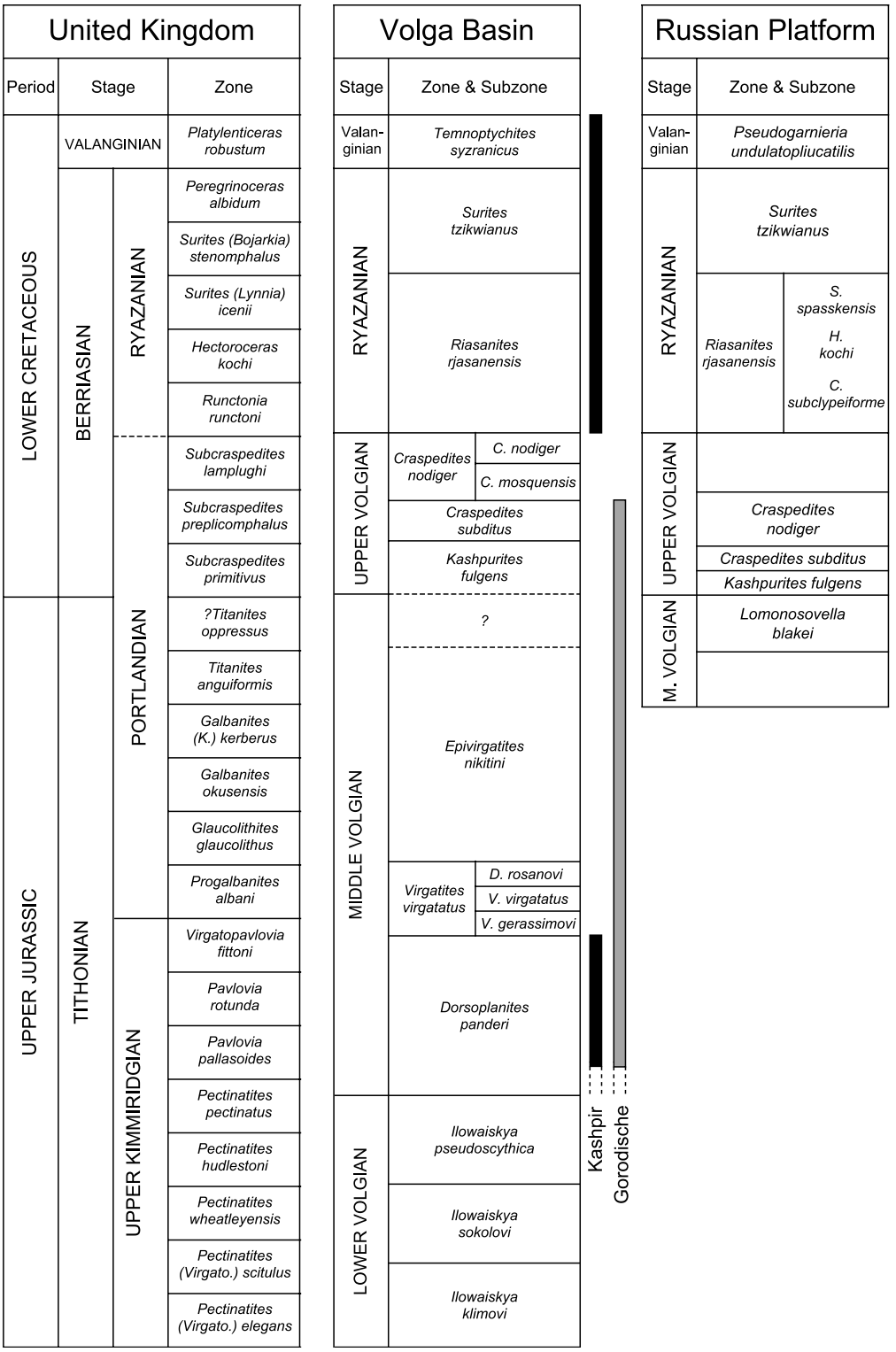
United Kingdom
Period
Stage
Zone
LOWER CRETACEOUS
VALANGINIAN
Platylenticeras robustum
BERRIASIAN
RYAZANIAN
Peregrinoceras albidum
Surites (Bojarkia) stenomphalus
Surites (Lynnia) icenii
Hectoroceras kochi
Runctonia runctoni
PORTLANDIAN
Subcraspedites lamplughi
Subcraspedites preplicomphalus
Subcraspedites primitivus
UPPER JURASSIC
TITHONIAN
?Titanites oppressus
Titanites anguiformis
Galbanites (K.) kerberus
Galbanites okusensis
Glaucolithites glaucolithus
Progalbanites albani
UPPER KIMMIRIDGIAN
Virgatopavlovia fittoni
Pavlovia rotunda
Pavlovia pallasoides
Pectinatites pectinatus
Pectinatites hudlestoni
Pectinatites wheatleyensis
Pectinatites (Virgato.) scitulus
Pectinatites (Virgato.) elegans
Volga Basin
Stage
Zone & Subzone
Valanginian
Temnoptychites syzranicus
RYAZANIAN
Surites tzikwianus
Riasanites rjasanensis
UPPER VOLGIAN
Craspedites nodiger
C. nodiger
C. mosquensis
Craspedites subditus
Kashpurites fulgens
MIDDLE VOLGIAN
?
Epivirgatites nikitini
Virgatites virgatatus
D. rosanovi
V. virgatatus
V. gerassimovi
Dorsoplanites panderi
LOWER VOLGIAN
Ilowaiskya pseudoscythica
Ilowaiskya sokolovi
Ilowaiskya klimovi
Kashpir
Gorodische
Russian Platform
Stage
Zone & Subzone
Valanginian
Pseudogarnieria undulatopliucatilis
RYAZANIAN
Surites tzikwianus
Riasanites rjasanensis
S. spasskensis
H. kochi
C. subclypeiforme
UPPER VOLGIAN
Craspedites nodiger
Craspedites subditus
Kashpurites fulgens
M. VOLGIAN
Lomonosovella blakei

Volga Basin was located at a palaeolatitude of 40–45°N (Fig. 1; Smith et al., 1994). Based on the palaeogeographic reconstructions of Sazonova and Sazanov (1967) and Baraboshkin (1997), land areas may have existed to the southwest and northeast of the study area, with marine connections to the Boreal and Tethyan seas. The width of the basin varied through time (Baraboshkin, 1997) but in the Late Berriasian it was about 500 km east to west and over 2000 km north to south. Intra-basinal 'highs' are common and these are thought to have provided some of the clastic sediment observed in the basin-fill. Post-depositional burial of the Mesozoic succession rarely exceeds a few hundred metres. Two outcrops were examined in the Volga Basin exposed adjacent to the River Volga (Fig. 2). The succession studied at Gorodische village (25 km north of Ulyanovsk) represents the stratotype of the Volgian (Gerasimov and Mikhailov, 1966) and ranges from the *Dorsoplanites panderi* Zone (Middle Volgian) to the *Craspedites nodiger* Zone (Upper Volgian; Fig. 3). The Gorodische succession, comprised of calcareous mudstones with four 0.5–1-m-thick black organic carbon-rich shale beds, is overlain by a thin (~2-m) silty-sand bed with abundant phosphatic nodules (Fig. 4). Invertebrates from this highly fossiliferous succession include belemnites, ammonites and bivalves (Kuleva et al., 1996; Hantzpergue et al., 1998). The Kashpir section (Fig. 5) is situated some 150 km south of the Gorodische type section (Fig. 2). A similar sedimentary succession to Gorodische is observed, whereby calcareous mudstones interbedded with thinner organic carbon-rich shale beds are overlain by a ~2-m phosphatic nodule-rich silty-sand bed. The lower part of this succession is dated on the basis of the ammonite fauna as Middle Volgian (*panderi–virgatus* Zones), whereas the upper section is Late Volgian to Early Valanginian (Hantzpergue et al., 1998; Baraboshkin, 1999). An isotopic study of Oxfordian belemnites from the Volga Basin has been made by Riboulleau et al. (1998).

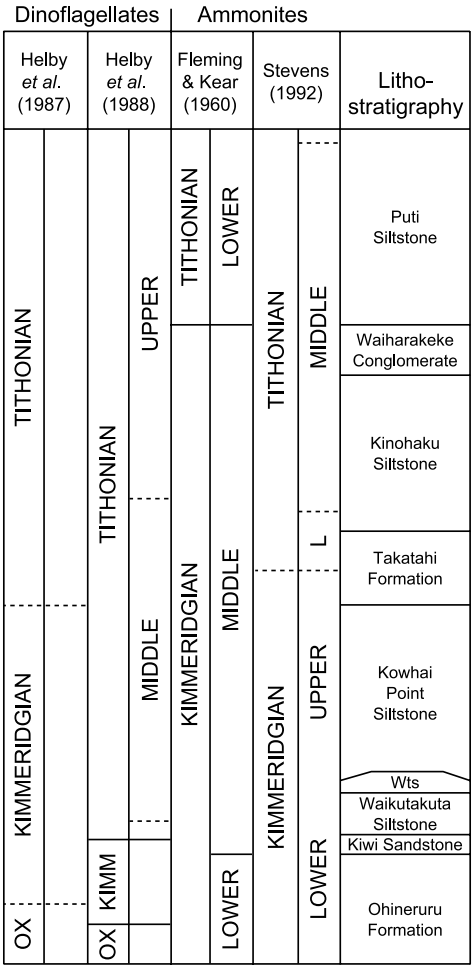

Fig. 4. The dinoflagellate and ammonite biostratigraphic schemes for Kawhia Harbour against lithostratigraphic units. Abbreviations: Ox, Oxfordian; Kimm, Kimmeridgian; L, Lower.

2.2. Kawhia Harbour, New Zealand

New Zealand was located during the Late Jurassic at a palaeolatitude of ~80°S (Fig. 1; Smith et al., 1994). Belemnite samples of Oxfordian–Tithonian age from Kawhia Harbour were provided by A.B. Challinor and are illustrated against a summarised stratigraphic section in Fig. 4 (Mesook and Grant-Mackie, 1995). Based upon the

Fig. 3. Ammonite biostratigraphic zonations of the Russian Platform and Volga Basin in comparison to the standard NW European ammonite zonal scheme (Casey, 1973; Casey and Rawson, 1973; Casey et al., 1977, 1988; Cope et al., 1980; Cope, 1995; Hancock, 1991; Hoedemaeker, 1991; Hantzpergue et al., 1998). Stratigraphic ranges of localities are shown.

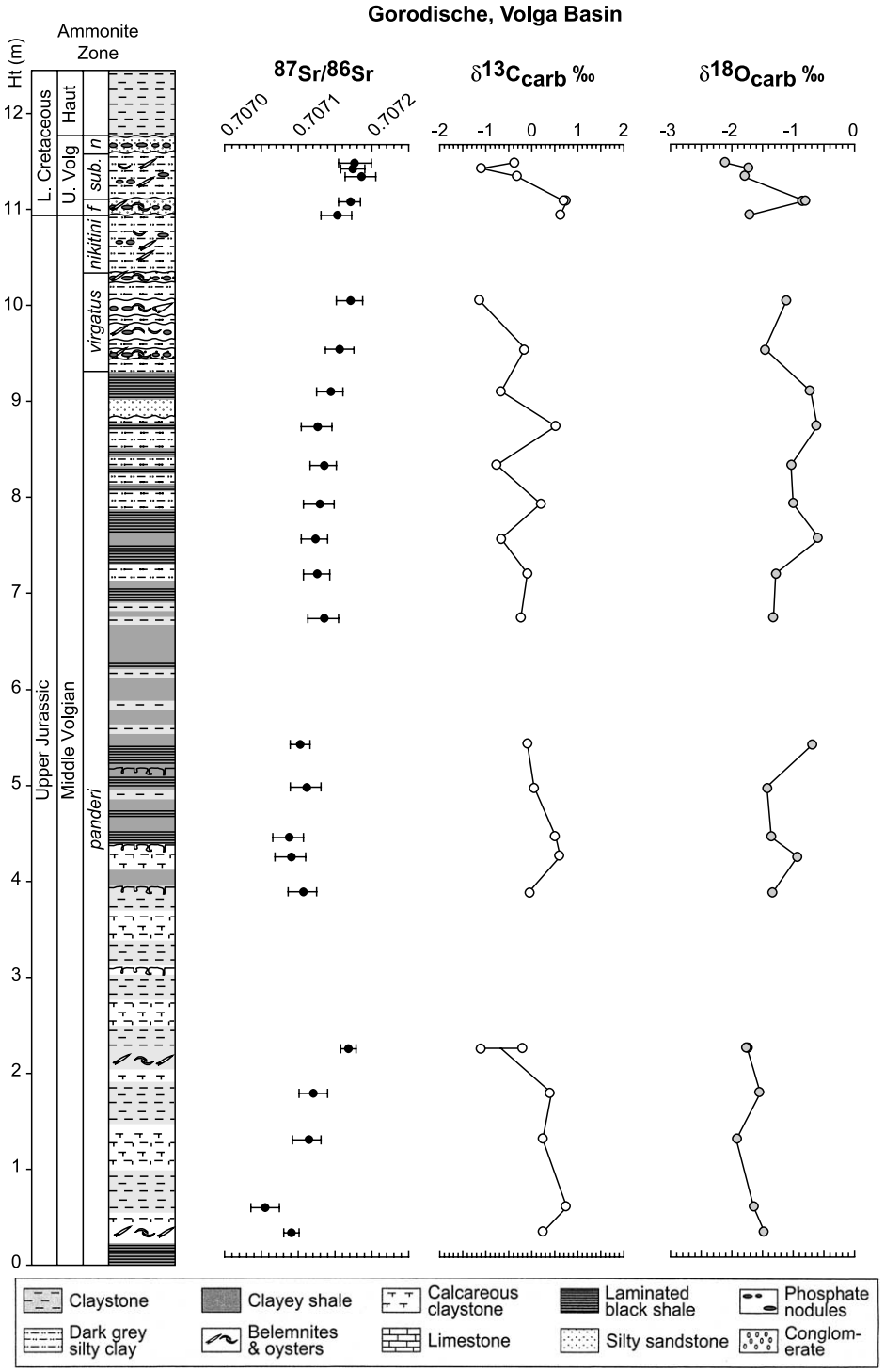

Fig. 5. Isotopic data from the Gorodische section, Volga Basin. Abbreviations: *f*, *fulgens*; *sub*, *subditus*; *n*, *nodiger*; Haut, Hauterivian; U. Volg, Upper Volgian.

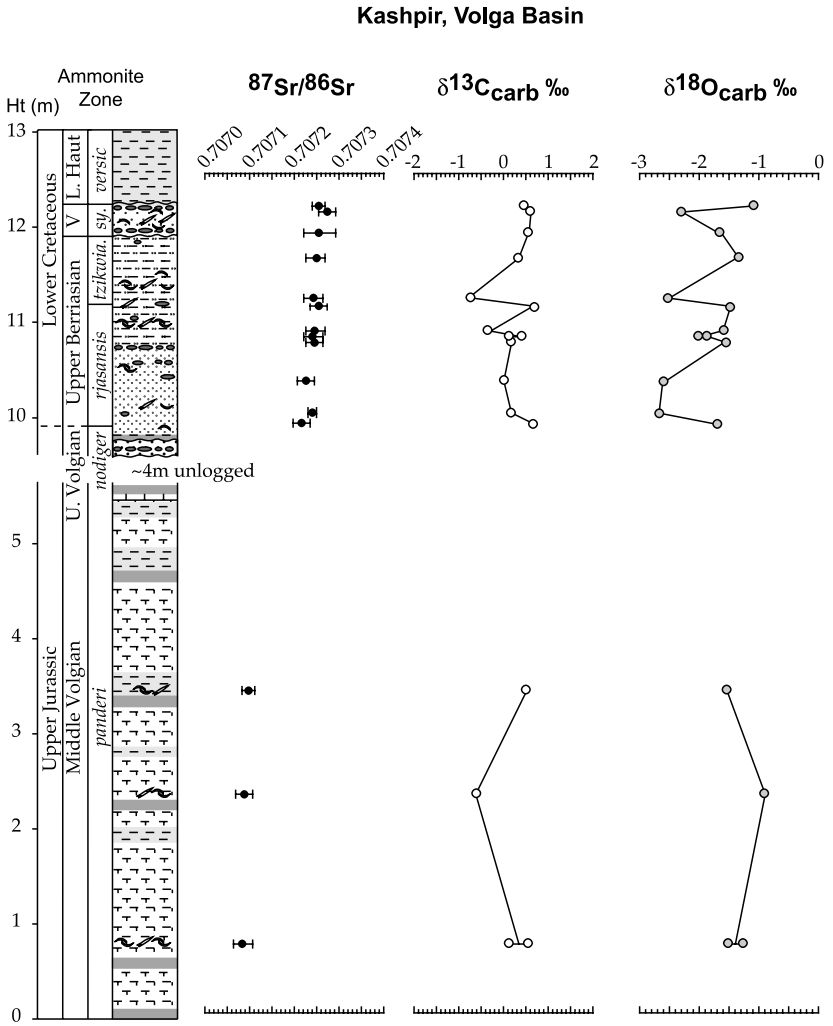

Fig. 6. Isotopic data from the Kashpir section, Volga Basin. Note the ~4 m of unlogged section due to poor exposure. Abbreviations: *sy*, *syzranicus*; *versic*, *versicosum*; U. Volg, Upper Volgian; V, Valanginian; L. Haut, Lower Hauterivian. Refer to Fig. 5 for lithological key.

lithostratigraphic scheme developed by Fleming and Kear (1960), the succession consists of eight formations (Fig. 6), ranging from siltstones to very fine sandstones, interspersed with conglomerates and calcareous concretions. The succession is extremely expanded and has a total thickness of ~4.6 km (Mesook and Grant-Mackie, 1995; Challinor, 1999).

2.3. Biostratigraphic correlation

The Jurassic and Cretaceous are characterised by a pronounced provinciality of ammonites within Europe (Casey and Rawson, 1973). Therefore, a number of parallel biostratigraphic schemes based upon ammonites have been erected. Ammonite provincialism became most pronounced in the latest Jurassic, with totally separate Boreal and Tethyan faunas (Cope, 1995). Different aspects of the Boreal fauna were identified for the Russian/Polish (Volgian) area and the British/Greenlandic Province (Cope, 1995). As the faunas are often so distinct, at present it is difficult to correlate between them and, hence, separate

stages are used for these areas: Tithonian in the Tethyan region, Volgian in the Russian areas and Portlandian in the British realm. The biostratigraphical resolution of the Jurassic is becoming progressively better (Cope, 1995) allowing for increasingly fine-scale biostratigraphic correlation. Although the sequence of ammonite zones (and subzones) can be convincingly replicated, the positions of the recognised stage boundaries based upon these zones are still variable and confusing (see Cope et al., 1980; Harland et al., 1990; Cope, 1995).

Numerous biostratigraphic schemes (e.g. Gerasimov, 1969; Casey, 1973; Casey et al., 1988; Baraboshkin, 1999; Hoedemaeker, 1995) have been erected for the Volgian of the Russian Platform based upon ammonites, and correlated with European schemes. Subsequenetly, Hantzpergue et al. (1998) developed an Upper Jurassic–Lower Cretaceous biostratigraphic scheme based upon ammonites from the Volga region, which is broadly comparable with that derived from the Russian Platform (Fig. 3). Hantzpergue et al. (1998) noted that the best biostratigraphical correlations between the Russian Platform and NW Europe were achieved for the Kimmeridgian where there are seven ammonite horizons in common between the two areas. However, despite increased biostratigraphical refinement, Hantzpergue et al. (1998) recognised that the equivalencies between the Volgian–Lower Cretaceous of Russia and Tithonian/Portlandian–Lower Cre-

Table 1
Isotopic and trace-element data from Gorodishe, Russia

Sample ID	Height (m)	Age (Ma)	$\delta^{13}C$ (‰)	$\delta^{18}O$ (‰)	Temperature (°C)	$^{87}Sr/^{86}Sr$	Fe (ppm)	Mn (ppm)
V1-1334	23.90	142.71	−0.39	−2.11	20.77	0.707180	21	2
V1-1314	23.80	142.85	−1.10	−1.70	18.95	0.707177	34	4
V1-1309	23.65	142.94	−0.31	−1.79	19.37	0.707187	16	6
V1-1274B	23.20	143.35	0.71	−0.79	15.13		49	2
V1-1274A	23.20	143.35	0.74	−0.84	15.34	0.707173	25	3
V1-1244	22.95	144.20	0.61	−1.71	19.01	0.707156	18	15
V1-1174	21.40	145.99	−1.13	−1.12	16.49	0.707172	10	1
V1-1154	20.50	146.71	−0.12	−1.47	17.95	0.707159	19	4
V1-1085	19.75	147.01	−0.67	−0.70	14.79	0.707146	24	9
V1-1035	19.10	147.05	0.52	−0.60	14.38	0.707128	37	5
V1-1015	18.40	147.11	−0.75	−1.02	16.10	0.707138	29	6
V1-975	17.70	147.15	0.20	−1.00	16.02	0.707130	19	11
V1-935	17.05	147.20	−0.68	−0.58	14.30	0.707126	9	10
V1-890	16.40	147.24	−0.07	−1.28	17.16	0.707128	25	3
V1-845	15.60	147.30	−0.26	−1.33	17.38	0.707137	21	9
V1-735	13.30	147.46	−0.08	−0.68	14.69	0.707103	35	2
V1-695	12.50	147.51	0.04	−1.44	17.84	0.707113	33	4
V1-640	11.60	147.57	0.51	−1.37	17.54	0.707090	18	16
V1-610	11.25	147.60	0.62	−0.91	15.63	0.707093	14	1
V1-585	10.60	147.65	−0.04	−1.33	17.36	0.707110	18	8
V1-455A	7.75	147.84	−1.11	−1.73	19.10	0.707171	21	7
V1-455B	7.75	147.84	−0.19	−1.76	19.23		22	9
V1-395	6.95	147.90	0.42	−1.53	18.21	0.707124	15	12
V1-345	6.10	147.96	0.23	−1.94	20.00	0.707115	28	9
V1-275	4.85	148.04	0.77	−1.64	18.70	0.707058	24	4
V1-255	4.40	148.07	0.27	−1.48	18.00	0.707094	31	2

Age determinations are based on Pálfy et al. (2000) preceding the Kimmeridgian–Tithonian boundary and Gradstein et al. (1995), thereafter assuming equal subzone duration as in Jones et al. (1994a,b). Stable-isotope ratios are expressed in per mil (‰) and against VPDB. Palaeotemperatures are determined assuming a δ_w value of seawater of −1‰ VSMOW (assuming an ice-free world). Strontium-isotope ratios have all been normalised to the NBS 987 value of 0.710250. Trace-element ratios expressed as parts per million (ppm).

taceous of NW Europe were much less certain; related to pronounced provincialism. Alternative biostratigraphic schemes published by Saks and Shulgina (1973) and Shulgina (1985, 1996) do show some significant differences and exclude the Upper Volgian as an equivalent of the Lower Berriasian, but place it as equivalent to the Upper Tithonian. In this study, the biostratigraphic scheme of Hantzpergue et al. (1998) will be used for correlating between the Russian sections and European ammonite zonal schemes.

Based upon the ammonite biostratigraphy of Fleming and Kear (1960), the estimated age of the Kawhia Harbour succession ranges from the Lower Kimmeridgian to the Upper Tithonian. Since then several studies have estimated ranges from the Upper Callovian to the Upper Tithonian, predominantly based on dinoflagellates (e.g. Helby et al., 1987, 1988). Recent correlation using ammonite biostratigraphy by Stevens (1992) suggests that the base of the Ohineruru Formation is basal Kimmeridgian, whereas the top of the Puti Siltstone is basal Upper Tithonian (Fig. 4). Belemnites were analysed from the base of the Ohineruru Formation to the Lower Puti Siltstone, and hence from Lower Kimmeridgian to the Middle Tithonian, using the scheme of Stevens (1992).

3. Analytical procedures

Carbonate staining following the method of Dickson (1966), electron microscopy and cathodoluminescence (CL) techniques were employed to characterise the state of preservation of each belemnite rostrum prior to isotopic and trace-element analysis. Subsequently, the outer surfaces of belemnites were removed using a circular grinder and thoroughly cleaned used deionised water and dried at room temperature. Avoiding areas where staining indicated ferroan carbonate or which were highly luminescent under CL, <5-mm fragments of the belemnite rostrum were selected and treated with 0.6 M HCl in FEP beakers and placed in an ultrasonic bath for $\sim$10 min. Samples were then rinsed with water, dried and broken into fragments <2 mm. After etching with 0.3 M HCl for $\sim$10 min (sustaining the reaction by drop-wise additions of 6 M HCl), samples were rinsed with water and dried.

3.1. Trace-element abundance

Approximately 20 mg subsamples were dissolved in concentrated HCl, added in stages allowing for any diffusive reactions to take place

Table 2
Isotopic and trace-element data from Kashpir, Russia

Sample ID	Height (m)	Age (Ma)	$\delta^{13}C$ (‰)	$\delta^{18}O$ (‰)	Temperature (°C)	$^{87}Sr/^{86}Sr$	Fe (ppm)	Mn (ppm)
K5-VT	19.40	135.65	0.50	−1.07	16.30	0.707257	15	2
K10-VT	19.30	135.78	0.63	−2.30	21.59	0.707277	19	6
K15-VT	18.90	136.37	0.57	−1.65	18.72	0.707259	32	1
K30-VT	18.45	137.10	0.31	−1.33	17.36	0.707251	24	5
K65-VT	17.70	137.38	−0.69	−2.54	22.69	0.707245	26	3
K70-VT	17.55	137.45	0.71	−1.47	17.96	0.707258	11	9
K100-VT	17.10	137.62	−0.34	−1.58	18.46	0.707249	13	10
K105-VTA	17.00	137.65	0.16	−1.87	19.69	0.707244	21	11
K105-VTB	17.00	137.65	0.44	−1.99	20.24		27	8
K110-VT	16.90	137.69	0.20	−1.52	18.17	0.707250	25	1
K150-VT	16.20	138.03	0.00	−2.61	23.01	0.707229	16	6
K170-VT	15.60	138.62	0.20	−2.67	23.27	0.707243	15	4
K175-VT	15.50	138.79	−0.73	−0.66	14.60		32	18
K180-VT	15.40	139.11	0.67	−1.71	18.98	0.707219	47	20
K-BB94	11.05	147.38	0.53	−1.54	18.25	0.707100	24	12
K-BB93	9.10	147.59	−0.62	−0.89	15.55	0.707092	12	6
K-BB91A	6.40	147.85	0.16	−1.50	18.11	0.707088	24	9
K-BB91B	6.40	147.85	0.55	−1.24	17.01		19	4

See Table 1 for column information.

in FEP beakers and subsequently brought up to 10 ml using deionised water. Elemental concentrations (Mn, Sr, Mg and Fe), shown in Tables 1–3, were determined by a Perkin Elmer 3000 inductively coupled plasma mass spectrometer. Reproducibility, based upon replicate analysis was calculated at less than ±5% of the measured concentration for Sr and Mg, and ±10% for Mn and Fe.

3.2. Strontium-isotope ratios

About 60 mg of the prepared belemnite rostrum was dissolved in 1–2-ml ~6 M HCl and the solution evaporated to incipient dryness. After re-dissolving the residue in 4 ml of 3.0 M HCl, the solution was transferred to a 15-ml tube and centrifuged. A 2-ml sample of the solution was loaded into a calibrated cation-exchange column equilibrated with 5 ml 3.0 M HCl. After washing the column with 19 ml 3.0 M HCl, the strontium was eluted in 8 ml 3.0 M HCl and evaporated to dryness.

0.5 μl 1.2 M H_3PO_4 was then placed in the centre of an out-gassed single tantalum filament followed by the sample strontium in 1 μl water. The solution was dried onto the filament by passing a current of ~1 amp. Finally, the current was increased momentarily until the filament became dull red to remove excess phosphoric acid and then turned off. Strontium-isotope measurements were performed on a modified VG Isomass 54 E thermal ionisation mass spectrometer. All $^{87}Sr/^{86}Sr$ values were internally normalised to a $^{86}Sr/^{88}Sr$ value of 0.1194. $^{87}Sr/^{86}Sr$ values, including other datasets, have been normalised to a National Bureau of Standards (NBS) 987 value of 0.710250.

3.3. Stable-isotope ratios

Samples prepared using the above procedure were powdered, measured out into thimbles and organic matter removed using 10% H_2O_2 for ~20 min after which time acetone was added to extract water. Samples were subsequently dried in an oven at 60°C. The samples were then loaded into a carousel with four internal standards, Carrara Marble, at the start and end of a run (i.e. eight standards and 36 samples). Isotopic analyses of belemnites were carried out using a VG PRISM Series II mass spectrometer with an on-line common acid-bath system at the University of Oxford. The $\delta^{18}O_{carb}$ and $\delta^{13}C_{carb}$

Table 3
Isotopic and trace-element data from Kawhia Harbour, New Zealand

Sample ID	Height (km)	Age (Ma)	$\delta^{13}C$ (‰)	$\delta^{18}O$ (‰)	Temperature (°C)	$^{87}Sr/^{86}Sr$	Fe (ppm)	Mn (ppm)
N51/F650	3.82	147.80	−0.13	0.36	10.59	0.707114	29	4
N51/F952	3.52	148.26	−0.54	−0.14	12.53	0.707093	12	2
N73/F630 A	3.33	148.52	−2.13	−1.90	19.83	0.707069	22	14
N73/F630 C	3.33	148.52	−1.17	−1.29	17.22	0.707066	25	8
N73/F628 A	3.25	148.65	−1.40	−0.52	14.04	0.707040	40	18
N73/F928 A	2.99	149.05	0.02	−0.39	13.53		14	11
N73/F928 B	2.99	149.05	−2.77	−0.50	13.97	0.707063	17	11
N73/F566	1.98	150.56	−0.10	−2.08	20.63	0.706983	34	4
N73/F69 A	1.66	151.64	0.31	−0.76	15.00		29	12
N73/F69 B	1.66	151.64	1.28	−0.71	14.79	0.706983	37	2
N73/F560 A	1.06	153.83	1.07	−2.07	20.58		21	9
N73/F560 B	1.06	153.83	0.29	−2.44	22.22	0.706897	17	9
N73/F560 C	1.06	153.83	0.83	−1.19	16.78	0.706875	12	3
N73/F556 A	0.43	154.57	0.65	−2.21	21.21	0.706843	15	5
N73/F556 B	0.43	154.57	0.74	−2.08	20.60		26	10
N73/F960 B	0.43	154.87	0.90	−3.10	25.26	0.706838	23	4
N73/F960 C	0.18	154.87	1.29	−2.66	23.24	0.706832	42	2

See Table 1 for column information.

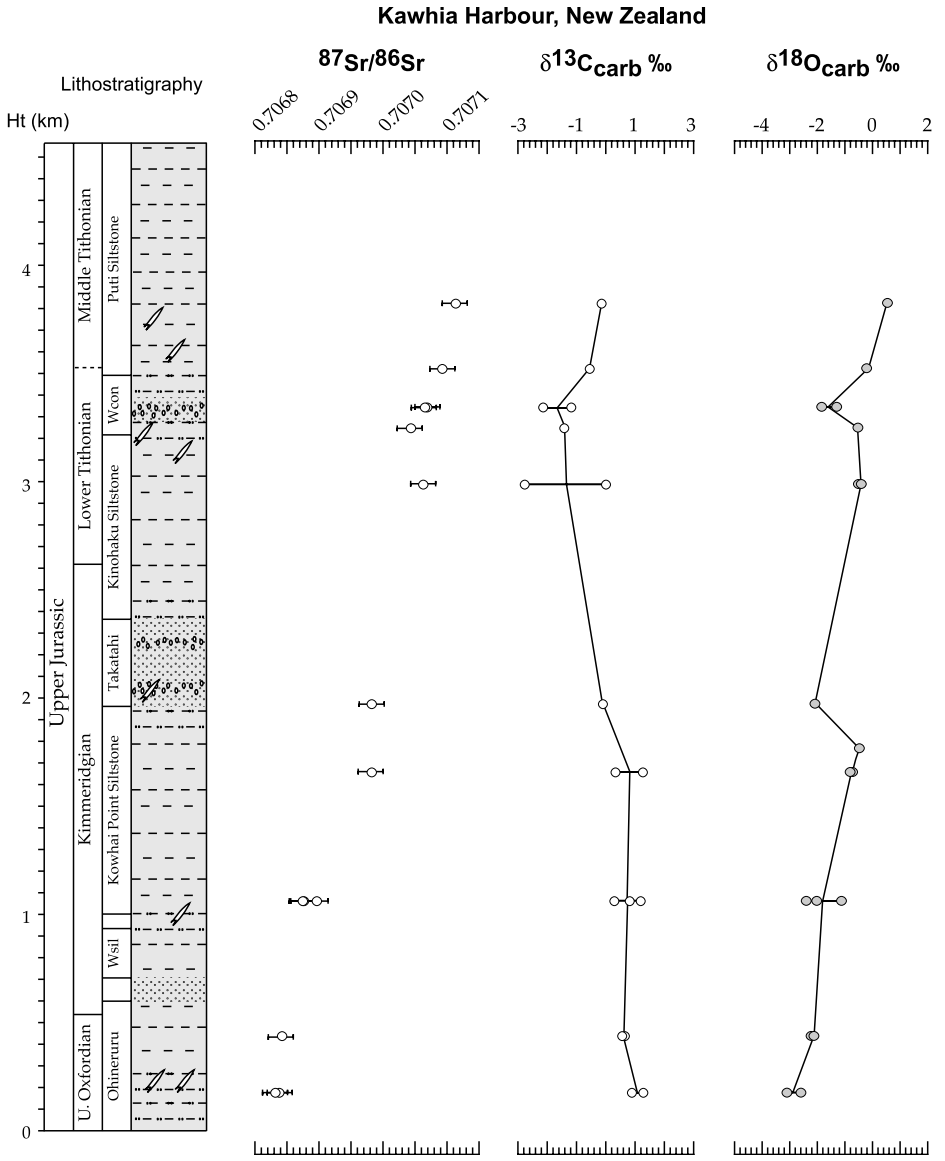

Fig. 7. Isotopic data from the Kawhia Harbour section, New Zealand. Refer to Fig. 5 for lithological key. Abbreviations: Wsil, Waikutakuta Siltstone; Wcon, Waiharakeke Conglomerate; U., Upper.

compositions are reported in per mil (‰) notation with respect to the Vienna PeeDee Belemnite (VPDB) international standard. Calibration of the isotopic results to VPDB was achieved via calibration of the Carrara Marble to NBS 19. Reproducibility of both $\delta^{18}O_{carb}$ and $\delta^{13}C_{carb}$ was generally better than ± 0.1‰ based on replicate analyses.

4. Results

4.1. Trace-element abundance and belemnite preservation

Trace-element variation has consistently been employed as a technique to identify diagenetic alteration (e.g. Brand and Veizer, 1980; Jones,

1992; Ditchfield et al., 1994; Jones et al., 1994a,b; Price and Sellwood, 1997; Podlaha et al., 1998; Hesselbo et al., 2000; Price et al., 2000; Gröcke, 2001; Jenkyns et al., 2002). Such studies indicate that high concentrations of Fe and Mn are commonly associated with more negative $\delta^{18}O$ and $\delta^{13}C$ values and sparry calcite resulting from diagenetic alteration. The measured concentrations of Mn in our material ranged from 3 to 205 ppm, Mg 431 to 1951 ppm, Sr 634to 1718 ppm and Fe 7 to 1131 ppm. Based on the study of modern marine molluscan shell carbonate (assumed to reflect pristine carbonate), relatively low concentrations of Mn (<100 ppm) and Fe (<200 ppm) are recorded, with Sr and Mg amounts proving more variable and in higher concentrations (e.g. Milliman, 1974; Morrison and Brand, 1986). Carbonate staining, cathodoluminescence and scanning-electron microscopic analysis reveal that the belemnites were mostly non-ferroan and non-luminescent, and retained the primary concentric banding that characterises belemnite rostra (Fig. 8). A number of samples, particularly those obtained from the silty-sand beds at Gorodische and Kashpir were weathered especially around the margins and commonly displayed partial replacement by phosphate preferentially along the concentric growth bands (Fig. 8). This latter feature may be due to the dissolution and subsequent cementation of unstable organic-rich layers within the rostrum. It is of note that the highest Fe and Mn values recorded are derived from those belemnites obtained from the silty-sand beds consistent with poor preservation observed in hand specimen and petrographic observations. Hence, where Fe and Mn values exceeded 200 and 100 ppm, respectively, these samples were excluded from further analysis in this study and are excluded from Tables 1–3.

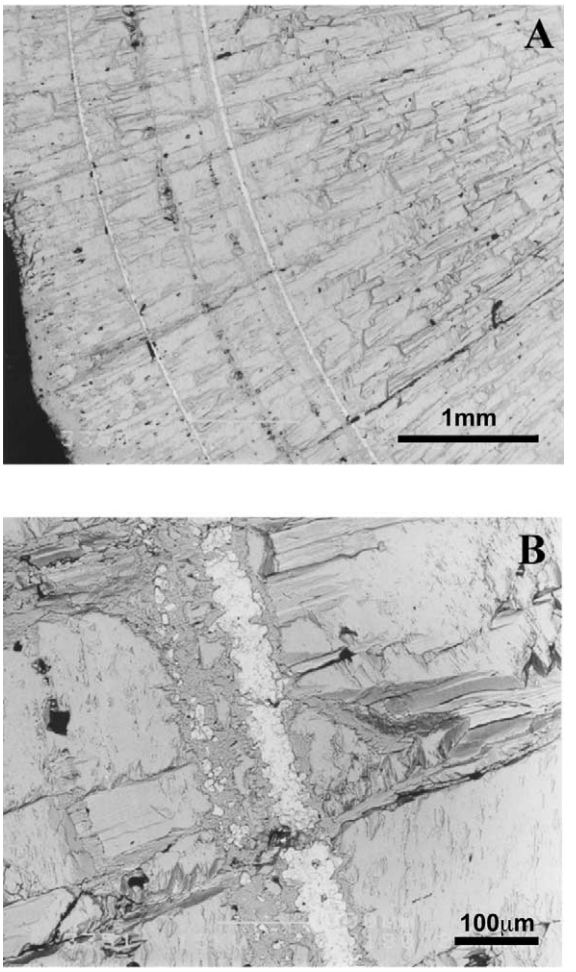

Fig. 8. (A) Back-scattered scanning electron photomicrograph showing partial replacement of belemnite rostrum by phosphate along concentric growth lines (scale bar = 1 mm). (B) A close-up image of the phosphate growth band (scale-bar = 100 μm).

4.2. Strontium-isotope ratios

$^{87}Sr/^{86}Sr$ values derived from the well-preserved belemnites at Gorodische (Fig. 5; Table 1) show some scatter in the lower *panderi* Zone during the deposition of calcareous clay-stones and may be related to pore-water diagenesis (Jones, 1992). However, when the succession changes to one dominated by clayey shales the $^{87}Sr/^{86}Sr$ values show very little variation, and gradually increase from the *Virgarites virgatus* Zone through to the *Craspedites subditus* Zone. A similar pattern is recognised from the Kashpir section (Fig. 6; Table 2) with relatively stable $^{87}Sr/^{86}Sr$ values from the *Kashpurites fulgens–nodiger* Zones and this extends into the *Temnoptychites syzranicus* Zone of the lower Valanginian. The Kawhia Harbour section records a gradual rise in $^{87}Sr/^{86}Sr$ values from

the Ohineruru Formation to the Puti Siltstone. As seen in Fig. 7, a close correspondence of the strontium-isotope ratios is observed between the data from this study and those of Podlaha et al. (1998).

4.3. Stable-isotope ratios

Where multiple belemnites were collected from the same stratigraphic level, the maximum variation in $\delta^{13}C_{carb}$ and $\delta^{18}O_{carb}$ is 0.9‰ and 0.2‰ from Gorodische and 0.4‰ and 0.2‰ from Kashpir, respectively. This is not the case for Kawhia Harbour, New Zealand. Where multiple belemnites are examined from a single horizon, the maximum variations in $\delta^{13}C_{carb}$ and $\delta^{18}O_{carb}$ are 3‰ and 1.2‰, respectively. It is interesting to note that oxygen-isotope variation is much smaller from all localities than that recorded for $\delta^{13}C_{carb}$ and may be related to ontogeny, variation in feeding habitats and/or stress-induced reabsorption of the rostrum.

The isotope profile from Gorodische (Fig. 5) shows a number of notable features. $\delta^{13}C_{carb}$ values remain fairly constant through the section, ranging from +0.77 to −1.13‰ (mean −0.06‰). $\delta^{18}O_{carb}$ values show a similar range from −0.58 to −2.11‰ (mean −1.30‰), with the most enriched values occurring in the uppermost part of the *panderi* Zone (Fig. 5; Table 1). At Kashpir $\delta^{13}C_{carb}$ values also exhibit a fairly narrow range (+0.67 to −0.73‰, mean +0.16‰), whilst oxygen isotope values range from −0.66 to −2.67‰ (mean −1.68‰) (Fig. 6; Table 2). In contrast, the isotopic data from Kawhia Harbour show much greater variation. $\delta^{18}O_{carb}$ values range from +0.36 to −3.09‰ (mean −1.39‰) and $\delta^{13}C_{carb}$ values range from +1.29 to −2.77‰ (mean −0.05‰)(Table 3). The greatest variation occurs in the Oxfordian–Kimmeridgian part of the sequence, whilst a narrower variation and a move towards more positive $\delta^{18}O_{carb}$ values are recorded in the upper (Tithonian) part of the succession (Fig. 7). A comparable isotopic range has previously been reported (Stevens and Clayton, 1971), although the belemnites used in that study were not fully screened for diagenetic alteration.

5. Discussion

5.1. Strontium-isotope variation and stratigraphic correlation

Fig. 9 illustrates the strontium-isotope data plotted against the emerging reference curve for the global evolution of marine strontium isotope ratios during the Late Jurassic–Early Cretaceous, based on belemnites collected from England (Jones et al., 1994a,b; Gröcke, 2001) and the Moscow Basin, Russia (Podlaha et al., 1998; Gröcke, 2001). The strontium-isotope data from the Volga Basin confirm the findings of Hantzpergue et al. (1998) based upon the affinities of endemic ammonites, that the *Dorsoplanites panderi* Zone is correlated with the Middle Tithonian ammonite faunal scheme from Europe. The data also support the proposition of the Upper Volgian as an equivalent of the Lower Berriasian at Kashpir (cf. Saks and Shulgina, 1973; Shulgina, 1985, 1996). Furthermore, as noted above, although the published data show a degree of scatter, the new data confirm the uniform rise in $^{87}Sr/^{86}Sr$ values from the Late Jurassic into the Early Cretaceous. However, the Early Cretaceous portion of the curve is appreciably flatter compared with the Late Jurassic (Fig. 9).

The Kawhia Harbour section records a gradual rise in $^{87}Sr/^{86}Sr$ values from the Ohineruru Formation to the Puti Siltstone (Fig. 7; Table 3). In comparison with the published $^{87}Sr/^{86}Sr$ curve derived from belemnites and oysters (Fig. 9), the strontium-isotope data from Kawhia Harbour suggest the lower part of the section (Ohineruru Formation) is latest Oxfordian in age as previously indicated by Helby et al. (1987) based on dinoflagellate biostratigraphy. This is not in agreement with the ammonite biostratigraphy of Stevens (1992) who suggests an Early Kimmeridgian age. However, it should be stressed that the $^{87}Sr/^{86}Sr$ values for the upper part of the section correlate well with the biostratigraphic correlation suggested by both Stevens (1992) and Helby et al. (1987): Lower–Middle Tithonian (Fig. 4). Therefore, it seems that correlation based on $^{87}Sr/^{86}Sr$ values is not significantly different from individual reports, but rather a combination of biostrati-

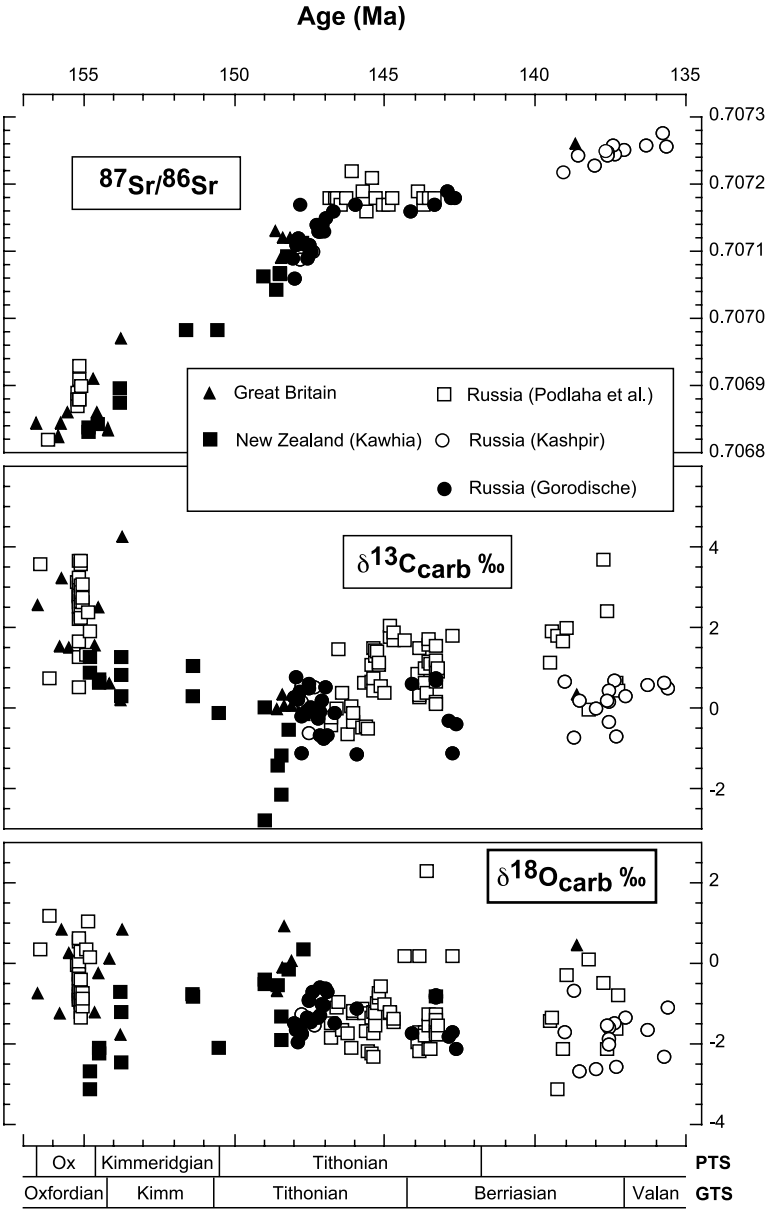

Fig. 9. Strontium-, carbon- and oxygen-isotope curves for the latest Oxfordian–earliest Valanginian data excluding diagenetically altered samples (data from this study and Jones, 1992; Jones et al., 1994a,b; Podlaha et al., 1998; Gröcke, 2001; Jenkyns et al., 2002), against the timescales of Pálfy et al. (2000) [PTS] and Gradstein et al. (1995) [GTS]. Abbreviations: Ox, Oxfordian; Kimm, Kimmeridgian; Valan, Valanginian.

graphic approaches (e.g. Helby et al., 1987; Stevens, 1992). The correlation based on strontium-isotope ratios as depicted in Fig. 4 with the NW European ammonite scheme has been used in this study for constructing the carbon- and oxygen-isotope curves for the Late Jurassic (Fig. 9).

It has recently been proposed by Jones and Jenkyns (2000) that hydrothermal activity/mid-oceanic ridge spreading was the dominant mech-

anism controlling seawater $^{87}Sr/^{86}Sr$ values for the Jurassic and Early Cretaceous. During the Cenozoic, continental weathering due to Himalayan uplift and erosion has been suggested as the dominant mechanism (Palmer and Elderfield, 1985; Hess et al., 1986; Derry and France-Lanord, 1996). The major mountain building period in the Jurassic and Early Cretaceous was the development of the Western Cordillera (Rocky Mountains). Stratigraphic, sedimentological and geochronological evidence tends to suggest an onset age during the Middle Jurassic (Archibald et al., 1983; Monger, 1998), although by the Late Jurassic large volumes of continental detritus was being deposited in the region compared to one previously dominated by marine sedimentation (Poulton, 1989).

Archibald et al. (1983) on the basis of K–Ar geochronology indicate that an uplift of ~7 km in the Western Cordillera began at ~156 Ma at a rate of 2 mm/yr, and an end age of ~152.5 Ma. Based on the timescale of Pálfy et al. (2000), the uplift event occurred during the Oxfordian–Kimmeridgian. $^{87}Sr/^{86}Sr$ values rise across the Oxfordian–Kimmeridgian boundary and continue for the remainder of the Late Jurassic, plateau across the Jurassic-Cretaceous boundary and start to rise again through the Early Cretaceous (Fig. 9), at least until the Late Barremian when they descend again (Gröcke, unpublished data). This trend in seawater strontium-isotope ratios would possibly indicate that the Western Cordillera mountain building event led to an increase in $^{87}Sr/^{86}Sr$ values similar to that in the Cenozoic. A decrease in weathering (as indicated by the strontium-isotope plateau) across the Jurassic-Cretaceous boundary is concordant with clay mineral data from NW Europe (Ruffell et al., 2002). However, this does not dismiss the premise that a decrease also occurred in mid-oceanic ridge spreading and/or hydrothermal flux. Both of these mechanisms (weathering and hydrothermal activity) may be inherently linked and, thus, the $^{87}Sr/^{86}Sr$ values represent a balance (a plateau in the strontium-isotope curve) or imbalance (rise or decline in the strontium-isotope curve). This may especially be the case since Sheridan (1997) reports that seafloor spreading in the Atlantic decreased from ~3.8 cm/yr in the Late Kimmeridgian to only ~1.5 cm/yr in the Late Tithonian.

5.2. Late Jurassic palaeotemperatures

The oxygen isotope record (Figs. 5–7) displays considerably more variability than the strontium-isotope record (particularly from New Zealand). This is likely to be related to the longer residence time associated with strontium in seawater (see McArthur, 1994), and the range of controls upon the $^{18}O/^{16}O$ value of carbonate which includes seawater temperature, vital effects and global next to localised variations in the isotopic composition of seawater (see Zeebe, 2002). In general, the $^{18}O/^{16}O$ ratio in seawater is decreased in response to precipitation and/or runoff whereas the $^{18}O/^{16}O$ ratio is increased by evaporation, and hence, in high latitudes where precipitation generally exceeds evaporation waters tend to be isotopically lighter. Furthermore, if ^{16}O-enriched water from ice and/or snow enters the oceanic system, this would result in more negative $\delta^{18}O_{carb}$ values and, thus, if interpreted in terms of palaeotemperature these values will give erroneously high estimates. Assuming that the isotopic composition of belemnites represents primary marine signatures (i.e. no or very little diagenetic alteration), calcite palaeotemperatures can be calculated using the equation of Epstein et al. (1953) and Craig (1965), and modified by Anderson and Arthur (1983). This expresses the oxygen-isotope composition of calcite (δ_c) with respect to VPDB, which is directly related to the oxygen-isotope composition of seawater (δ_w) in which the calcite precipitated with respect to VSMOW:

$$\text{Palaeotemperature } (^\circ\text{C}) = 16.0 - 4.14\,(\delta_c - \delta_w) + 0.13\,(\delta_c - \delta_w)^2$$

Using a δ_w value of −1.0‰ VSMOW, deemed appropriate for an ice-free world post-Jurassic time (Shackleton and Kennett, 1975; Lecuyer and Allemand, 1999; see below), calculated palaeotemperatures from the $\delta^{18}O_{carb}$ values are presented in Tables 1–3. Illustrated in Fig. 9 are

Table 4
Published belemnite-derived oxygen-isotope ratios for the Late Jurassic

Region	No.	$\delta^{18}O$ (‰)	Temperature* (°C)	Age	Reference	Fig. 10
Svalbard			5–11°C (8.0°C)	Tithonian–Valanginian	Ditchfield (1997)	1
Milne Land, East Greenland	5	−1.13 to −1.91 (−1.47)	17–20°C (18.0°C)	Middle Kimmeridgian–Tithonian	Bowen (1966)	2
Volga Basin	30	−0.58 to −2.11 (−1.30)	14–21°C (17.3°C)	Tithonian	This study	3
Hundsrück, Germany	9	−0.91 to −1.18 (−1.02)	16–17°C (16.1°C)	Early Kimmeridgian	Bowen (1961)	4
Lubaczow, Poland	4	−2.27 to −2.56 (−2.42)	22–23°C (22.1°C)	Late Jurassic	Bowen (1961)	4
Mallorca, Spain	6	+0.04 to −1.00 (−0.48)	12–16°C (13.9°C)	Kimmeridgian–Tithonian	Price and Sellwood (1994)	5
Cutch, India	4	−0.40 to −0.59 (−0.46)	13–15°C (13.8°C)	Kimmeridgian	Bowen (1966)	6
Santa Cruz, Argentina	4	−1.60 to −2.00 (−1.90)	19–20°C (19.8°C)	?Tithonian	Bowen (1961)	7
Falkland Plateau	24	−0.95 to −1.88 (−1.38)	16–20°C (17.6°C)	Oxfordian–Tithonian	Price and Sellwood (1997)	7
James Ross Island	8	−0.26 to −1.02 (−0.67)	13–16°C (14.6°C)	Tithonian	Ditchfield et al. (1994)	8
Kawhia Harbour, New Zealand	17	−3.10 to +0.36 (−1.39)	11–25°C (17.8°C)	Upper Oxfordian–Middle Tithonian	This study	9

Palaeotemperatures have been calculated using the equation of Anderson and Arthur (1983) and a δ_w of −1.0 (VSMOW).

$\delta^{18}O_{carb}$ values from this study, combined with published belemnite data for the Late Jurassic–Early Cretaceous interval: a warming through the Oxfordian–Kimmeridgian, cooler palaeotemperatures within the Early Tithonian and a gradual rise to warmer palaeotemperatures across the Jurassic–Cretaceous boundary.

The observed palaeotemperature range from the Volga Basin (14–23°C: mean ~18°C) is similar to calculated Late Jurassic belemnites from East Greenland (Bowen, 1966) and Poland (Teys et al., 1968; Bowen, 1961) (Table 4), but are considerably warmer than those reported by Ditchfield (1997) who proposes a palaeotemperature range of ~5–11°C (mean: ~8°C) for the Tithonian–Valanginian based on belemnites from Svalbard (palaeolatitude 65°N). It is likely there was ~25° of latitudinal difference between the Volga Basin (40°N) and Svalbard during the Late Jurassic. Using average palaeotemperatures, a gradient of ~0.36°C is calculated for every degree of palaeolatitude, which if extrapolated to northern polar regions may indicate sub-freezing palaeotemperatures at a palaeolatitude greater than ~80°N. A palaeotemperature gradient of ~3.6°C per every 10° of latitude is comparable to the ~3°C proposed by Pirrie and Marshall (1990) for the Late Cretaceous.

The palaeotemperature estimates for Russia and other locations in northern Europe are paradoxically considerably warmer than those derived from more equatorial latitudes such as Mallorca and India (Table 4; Fig. 10 and inset). These cooler palaeotemperature estimates are for more open-marine settings and may be related to major circulation patterns in the Tethys Ocean, and/or increased upwelling of cold nutrient-rich bottom waters along the southern continental margins.

The calculated palaeotemperature range (11–25°C, mean ~18°C) for the New Zealand belemnite isotope data is relatively large (Fig. 10). In contrast, palaeotemperature estimates from high-latitude Southern Hemisphere locations, such as James Ross Island (Ditchfield et al., 1994), Argentina (Bowen, 1961) and the Falkland Plateau (Price and Sellwood, 1997; Price and Gröcke, 2002), all show a considerably narrower range of temperatures (Table 4). One possibility is that

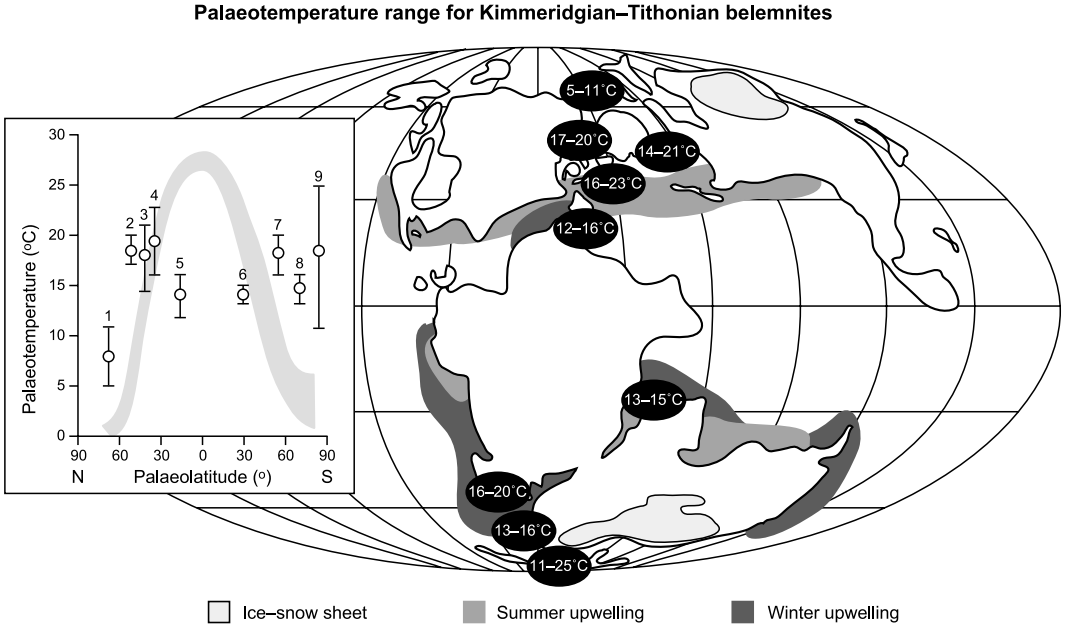

Fig. 10. Belemnite palaeotemperatures for the Kimmeridgian–Tithonian interval illustrated on the palaeogeographic map of Fig. 1. Palaeotemperature estimates are derived from this study and data within Table 4. Numbers within inset refer to Table 4 and shaded curve represents a modern pole-to-pole sea-surface temperature profile from Smith et al. (1996). Postulated ice/snow-sheets are from Sellwood et al. (2000), zones of upwelling from Parrish and Curtis (1982) and Price et al. (1995).

the variability seen in the $\delta^{18}O_{carb}$ values from New Zealand is a consequence of localised variations in the isotopic composition of the seawater. The most negative $\delta^{18}O_{carb}$ values representing the most elevated palaeotemperatures recorded in the lowermost Kimmeridgian may be indicative of the input of ^{16}O-enriched water resulting from a reduction in ice and/or snow-sheet and associated increased runoff (Sellwood et al., 2000). Given the magnitude of the ice/snow-sheet proposed by Sellwood et al. (2000), it is unlikely to have had an affect on the global $\delta^{18}O$ value of seawater. The return towards more 'realistic' marine palaeotemperatures expected for the palaeolatitude of New Zealand during the Lower–Middle Tithonian points to a reduction in the ice/snow-runoff factor (Fig. 9). Based on the Middle Tithonian palaeotemperatures from New Zealand, of ~11°C, and assuming similar palaeotemperature gradients between the Northern and Southern Hemispheres, this would indicate that the ice/snow-sheet had little affect on $\delta^{18}O_{carb}$ values for that time period.

5.3. The Late Jurassic–Early Cretaceous $\delta^{13}C_{carb}$ curve

Illustrated in Fig. 9 are $\delta^{13}C_{carb}$ values from this study, combined with published belemnite data for the Late Jurassic–Early Cretaceous interval. A sharp decrease from +3.5‰ in the Upper Oxfordian to −2.5‰ in the Middle Tithonian is observed. From these lowest values in the Middle Tithonian, $\delta^{13}C_{carb}$ values generally rise to ~+2‰ just prior to the Jurassic–Cretaceous boundary based on the Gradstein et al. (1995) timescale. $\delta^{13}C_{carb}$ ratios decline after the Jurassic–Cretaceous boundary and continue to decline until the Lower Berriasian where $\delta^{13}C_{carb}$ values begin to fluctuate with some extremely positive values in the Upper Berriasian (~+4‰).

Bartolini et al. (1999) examining Tethyan sections also documented a major positive $\delta^{13}C_{carb}$ excursion to values of ~+4‰ in the Middle–Upper Oxfordian and further report that $\delta^{13}C_{carb}$ values decrease almost systematically through to the Lower Tithonian. The general de-

crease in $\delta^{13}C_{carb}$ has also been noted by Weissert and Mohr (1996) and Weissert et al. (1998), and more recently by Padden et al. (2002). Although the positive shift from the Lower–Middle Tithonian to the Jurassic–Cretaceous boundary has not been previously reported, some indications of it may be seen at Valle del Mis, Belluno Basin (Weissert and Channell, 1989). Because these patterns in $\delta^{13}C_{carb}$ are documented in both the Northern and Southern Hemispheres, this suggests that the carbon reservoir was ultimately controlled by global rather than local and/or regional environmental conditions. Weissert and Channell (1989) and Weissert and Mohr (1996) suggest that the positive carbon-isotope events in the Late Jurassic relate to increased organic-carbon accumulation rates and changing efficiency of the oceanic carbonate-carbon pump. Weissert and Mohr (1996) further suggest that intensified Late Jurassic water-cycling, triggered by elevated levels of atmospheric CO_2, led to enhanced chemical weathering in a warm and humid environment leading to increased erosion and nutrient transfer from the continents to oceans. Clay-mineral assemblages (i.e. Ruffell and Rawson, 1994) and strontium-isotope evidence also tend to support an increase in weathering rates in the Late Jurassic.

6. Conclusions

$^{87}Sr/^{86}Sr$ values derived from well-preserved belemnites from the Volga Basin confirm the findings of Hantzpergue et al. (1998) that the *panderi* Zone is correlatable with the Middle Tithonian ammonite zonal from Europe, and the proposition of the Upper Volgian as an equivalent of the Lower Berriasian. Our data also confirm the uniform rise in $^{87}Sr/^{86}Sr$ values from the Late Jurassic into the Early Cretaceous, however, the gradient of the curve changes from being relatively steep in the Late Jurassic to markedly less so in the Early Cretaceous. The Kawhia Harbour section records a gradual rise in $^{87}Sr/^{86}Sr$ values and in comparison with the published $^{87}Sr/^{86}Sr$ curve suggests that the lower part of the section is latest Oxfordian in age as previously indicated by Helby et al. (1987). The $^{87}Sr/^{86}Sr$ values for the upper part of the section correlate well with the biostratigraphic correlation suggested by both Stevens (1992) and Helby et al. (1987): Lower–Middle Tithonian.

The oxygen-isotope data from Russia if interpreted in terms of palaeotemperature provide a range from 14 to 23°C (mean ~18°C) and are consistent with a slight cooling through the Middle Volgian and warmer temperatures during the Late Volgian–Early Ryazanian. If extrapolated to Northern Hemisphere regions, the data may indicate sub-freezing palaeotemperatures at a palaeolatitude greater than ~80°N. In contrast, the calculated palaeotemperature range (11–25°C, mean ~18°C) for the New Zealand belemnite isotope data shows a much greater range. Combining these data with published studies, several distinguishing features are apparent: (1) moderately warm palaeotemperatures for mid-palaeolatitude localities (40–50°N) located in seaways; (2) generally elevated palaeotemperatures in the Southern Hemisphere compared to the same palaeolatitude in the Northern Hemisphere; (3) open-ocean localities (Mallorca and India) generally have lower palaeotemperatures compared to northern mid-palaeolatitude localities; and (4) extremely variable palaeotemperatures for the South Pole region (New Zealand).

The variability in the New Zealand data is interpreted to be a consequence of localised and intermittent input of ^{16}O-enriched water resulting from a reduction in an ice/snow-sheet and increased runoff. This is consistent with recent General Circulation Model results (Sellwood et al., 2000), which indicate that Antarctica and Australia may have sustained an ice/snow-sheet during the Oxfordian–Middle Tithonian. Thus, the semi-arid climate associated with the Late Jurassic may have been interspersed with cool climatic phases and/or the decline of a major cold phase associated with the development of an ice/snow-sheet in the Southern Hemisphere. More enigmatic is the general decline to very negative $\delta^{13}C_{carb}$ values over the Kimmeridgian–Early Tithonian that is associated with a gradual warming trend. This may indicate poor oceanic circulation and/or upwelling of nutrient-rich cold bottom waters (Küs-

pert, 1982) in the Tethys Ocean. The precise mechanism behind decreased organic-carbon burial rates and low carbon-isotope values in the Late Jurassic may relate inherently to increased continental weathering and subsequent lowering of global CO_2 levels to the Hauterivian-Barremian boundary (Robinson et al., 2002). Such a situation creates a paradox in that increased continental weathering should be linked with increased nutrient supply to the oceans and subsequent oceanic productivity and major positive carbon-isotope events.

Acknowledgements

D.R.G. was funded by Esso UK. Many thanks are due to Stephen Hesselbo and Hugh Jenkyns for discussions. This study was funded by a Royal Society Travel Grant (G.D.P. and A.H.R.) and the Deutsche Forschungsgemeinschaft (Mu667/14-1). We are grateful for the technical support provided by the University of Plymouth, The Queens University of Belfast and the University of Oxford. Larry Frakes, Uwe Brand and Finn Surlyk are thanked for putting a great deal of effort into reviewing this manuscript, and improving it immensely.

References

Anderson, T.F., Arthur, M.A., 1983. Stable isotopes of oxygen and carbon and their application to sedimentologic and environmental problems. In: Arthur, M.A., Anderson, T.F., Kaplan, I.R., Veizer, J., Land, L.S. (Eds.), Stable Isotopes in Sedimentary Geology. Soc. Econ. Paleontol. Mineral. Short Course Notes 10, 1.1–1.151.

Anderson, T.F., Popp, B.N., Williams, A.C., Ho, L.Z., Hudson, J.D., 1994. The stable isotopic records of fossils from the Peterborough Member, Oxford Clay Formation (Jurassic), UK: Palaeoenvironmental considerations. J. Geol. Soc. Lond. 151, 125–138.

Archibald, D., Glover, J.K., Price, R.A., Farrar, E., Carmichael, D.M., 1983. Geochronology and tectonic implications of magmatism and metamorphism, southern Kootenay arc and neighbouring regions, southestern British Columbia, Part 1. Jurassic to mid-Cretaceous. Can. J. Earth Sci. 20, 1891–1913.

Baraboshkin, E.J., 1997. The Tethyan/Boreal problem as the result of paleobiogeographical changes: Early Cretaceous examples from the Russian Platform. Mineralia Slovaca 29, 250–252.

Baraboshkin, E.J., 1999. Berriasian–Valanginian (early Cretaceous) seaways of the Russian Platform Basin and the problem of Boreal/Tethyan correlation. Geol. Carpath. 50, 5–20.

Bartolini, A., Baumgartner, P.O., Guex, J., 1999. Middle and Late Jurassic radiolarian palaeoecology versus carbon-isotope stratigraphy. Palaeogeogr. Palaeoclimatol. Palaeoecol. 145, 43–60.

Bowen, R., 1961. Paleotemperature analysis of belemnoidea and Jurassic paleoclimatology. J. Geol. 69, 309–320.

Bowen, R., 1966. Paleotemperature Analysis. Elsevier, Amsterdam.

Brand, U., Morrison, J.O., 1987. Paleoscene No. 6: Biogeochemistry of fossil marine invertebrates, Geosci. Can. 14, 85–107.

Brand, U., Veizer, J., 1980. Chemical diagenesis of a multicomponent carbonate system-1: Trace elements. J. Sediment. Petrol. 50, 1219–1236.

Casey, R., 1973. The ammonite succession at the Jurassic–Cretaceous boundary in East England. In: Casey, R., Rawson, P.F. (Eds.), The Boreal Lower Cretaceous. Geol. J. 5, 196–266.

Casey, R., Rawson, P.F., 1973. A review of the Boreal Lower Cretaceous. In: Casey, R., Rawson, P.F. (Eds.), The Boreal Lower Cretaceous. Geol. J. 5, 131–145.

Casey, R., Mesezhnikov, M.S., Shulgina, N.I., 1977. Sopostavlonie pogranichnykh otlozhenii iury i mela anglii, Russkoi Platformy, pripoliarnogo Urala i Sibiri [Correlation of the Jurassic–Cretaceous boundary deposits of England, the Russian Platform, the Subarctic Urals and Siberia]. Izvestiia Akademii Nauk SSSR, Seriia Geologicheskaia (Proc. Acad. Sci. USSR, ser. geol.) 7, 14–33.

Casey, R., Mesezhnikov, M.S., Shulgina, N.I., 1988. Ammonitivye zony pogreanitchnykh otlojenij jury i mela v boreal'noj oblasti. Izvestiia Akademii Nauk SSSR, Seriia Geologicheskaia (Proc. Acad. Sci. USSR, ser. geol.) 10, 71–84.

Challinor, A.B., 1999. Belemnite biostratigraphy of the New Zealand Late Jurassic Mangaoran (Early Puaroan) Substage and the Puaroan Stage revisited. N.Z. J. Geol. Geophys. 42, 369–393.

Cope, J.C.W., 1995. Introduction to the British Jurassic. In: Taylor, P.D. (Ed.), Field Geology of the British Jurassic. Geol. Soc. Lond., pp. 1–7.

Cope, J.C.W., Duff, K.L., Parsons, C.F., Torrens, H.S., Wimbledon, W.A., Wright, J.K., 1980. A correlation of Jurassic rocks in the British Isles, Part Two, Middle and Upper Jurassic. Geol. Soc. Lond. Spec. Rep. 15.

Craig, H., 1965. The measurement of oxygen isotope palaeotemperatures. In: Tongiorgi, E. (Ed.), Stable Isotopes in Oceanographic Studies and Palaeotemperatures. Consiglio Nazionale delle Richerche, Laboratorio di Geologia Nucleare, Pisa, pp. 161–182.

Derry, L.A., France-Lanord, C., 1996. Neogene Himalayan weathering history and river $^{87}Sr/^{86}Sr$: Impact on the marine Sr record. Earth Planet. Sci. Lett. 142, 59–74.

Dickson, J.A.D., 1966. Carbonate identification and genesis as revealed by staining. J. Sediment. Petrol. 36, 491–505.

Ditchfield, P.W., 1997. High northern palaeolatitude Jurassic–Cretaceous palaeotemperature variation: New data from Kong Karls Land, Svalbard. Palaeogeogr. Palaeoclimatol. Palaeoecol. 130, 163–175.

Ditchfield, P.W., Marshall, J.D., Pirrie, D., 1994. High latitude palaeotemperature variation: New data from the Tithonian to Eocene of James Ross island, Antarctica. Palaeogeogr. Palaeoclimatol. Palaeoecol. 107, 79–101.

Elderfield, H., 1986. Strontium isotope stratigraphy. Palaeogeogr. Palaeoclimatol. Palaeoecol. 57, 71–90.

Epstein, S., Buchsbaum, R., Lowenstam, H.A., Urey, H.C., 1953. Revised carbonate-water isotopic temperature scale. Geol. Soc. Am. Bull. 64, 1315–1326.

Fleming, C.A., Kear, D., 1960. The Jurassic sequence of Kawhia Harbour, New Zealand. N.Z. Geol. Surv. Bull. 67, 1–50.

Frakes, L.A., 1979. Climates through Geologic Time. Elsevier, Amsterdam.

Frakes, L.A., Francis, J.E., 1988. A guide to Phanerozoic cold polar climates from high latitude ice-rafting in the Cretaceous. Nature 333, 547–549.

Frakes, L.A., Francis, J.E., Syktus, J.I., 1992. Climate Modes of the Phanerozoic. Cambridge University Press, Cambridge.

Gerasimov, P.A., 1969. Upper Substage of the Volgian stage of the central part of the Russian Platform: The paleontological–stratigraphical and lithological study (in Russian). Nauka Publishers, Moscow.

Gerasimov, P.A., Mikhailov, N.P., 1966. Volgian stage and the geostratigraphical scale for the Upper series of the Jurassic System (in Russian). Izvestiya Akademiy Nauk SSSR, seriya Geologicheskaya 2, 118–138.

Gradstein, F.M., Agterberg, F.P., Ogg, J.G., Hardenbol, J., van Veen, P., Thierry, J., Huang, Z., 1995. A Triassic, Jurassic and Cretaceous timescale. In: Berggren, W.A., Kent, D.V., Aubry, M.-P., Hardenbol, J. (Eds.), Geochronology, Time Scales and stratigraphic correlation. SEPM Spec. Publ. 54, 95–128.

Gröcke, D.R., 2001. Isotope Stratigraphy and Ocean–Atmosphere Interactions in the Jurassic and Early Cretaceous. D.Phil. Thesis, University of Oxford.

Hallam, A., 1981. Facies interpretation and the stratigraphic record. Oxford, W.H. Freeman.

Hallam, A., 1985. A review of Mesozoic climates. J. Geol. Soc. Lond. 142, 433–445.

Hallam, A., 1994. An Outline of Phanerozoic Biogeography. Oxford University Press, Oxford.

Hallam, A., 2001. A review of the broad pattern of Jurassic sea-level changes and their possible causes in light of current knowledge. Palaeogeogr. Palaeoclimatol. Palaeoecol. 167, 23–37.

Hancock, J.M., 1991. Ammonite scales for the Cretaceous System. Cretac. Res. 12, 259–291.

Hantzpergue, P., Baudin, F., Mitta, A., Olferiev, A., Zakharov, V.A., 1998. The Upper Jurassic of the Volga basin: Ammonite biostratigraphy and occurrence of organic-carbon rich facies. Correlations between boreal–subboreal and submediterranean provinces. In: Crasquin-Soleau, S., Barrier, É. (Eds.), Peri-Tethys Memoir 4: Epicratonic Basins of Peri-Tethyan platforms. Mém. Mus. Natl. Hist. Nat. 179, 9–33.

Haq, B.U., Hardenbol, J., Vail, P.R., 1987. Chronology of fluctuating sea levels since the Triassic. Science 235, 1156–1167.

Hardenbol, J., Thierry, J., Farley, M.B., Jacquin, T., de Graciansky, P.-C., Vail, P.R., 1998. Mesozoic and Cenozoic sequence chronostratigraphic framework in European basins. In: de Graciansky, P.-C., Hardenbol, J., Jacquin, T., Vail, P.R. (Eds.), Mesozoic and Cenozoic Sequence Stratigraphy of European Basins. SEPM Spec. Publ. 60, 3–13.

Harland, W.B., Armstrong, R.L., Cox, A.V., Craig, L.E., Smith, A.G., Smith, D.G., 1990. A Geological Time Scale. Cambridge University Press, Cambridge.

Helby, R., Morgan, R., Partridge, A.D., 1987. A palynological zonation of the Australian Mesozoic. Mem. Assoc. Aust. Palaeontol. 4, 1–94.

Helby, R., Wilson, G.J., Grant-Mackie, J.A., 1988. A preliminary biostratigraphy of Middle to Late Jurassic dinoflagellate assemblages from Kawhia, New Zealand. Mem. Assoc. Aust. Palaeontol. 5, 125–166.

Hess, J., Bender, M.L., Schilling, J.-G., 1986. Evolution of the ratio of strontium-87 to strontium-86 in seawater from Cretaceous to Present. Science 231, 979–984.

Hesselbo, S.P., Meister, C., Gröcke, D.R., 2000. A potential global stratotype for the Sinemurian–Pliensbachian boundary (Lower Jurassic), Robin Hood's Bay, UK: Ammonite faunas and isotope stratigraphy. Geol. Mag. 137, 601–607.

Hoedemaeker, P.J., 1991. Tethyan–Boreal correlations and the Jurassic–Cretaceous boundary. News. Strat. 25, 37–60.

Hoedemaeker, P.J., 1995. Ammonite evidence for long-term sea-level fluctuations between the 2nd and 3rd-order in the Lowest Cretaceous. Cret. Res. 16, 231–241.

Jenkyns, H.C., 1999. Mesozoic anoxic events and palaeoclimate. Zent.bl. Geol. Paläontol. 1997, 943–949.

Jenkyns, H.C., Jones, C.E., Gröcke, D.R., Hesselbo, S.P., Parkinson, D.N., 2002. Chemostratigraphy in the Jurassic System: Applications, limitations and implications for palaeoceanography. J. Geol. Soc. Lond. 159, 351–378.

Jones, C.E., 1992. Strontium Isotopes in Jurassic and Early Cretaceous Seawater. D.Phil. Thesis, University of Oxford.

Jones, C.E., Jenkyns, H.C., 2000. Seawater strontium isotopes, oceanic anoxic events, and seafloor hydrothermal activity in the Jurassic and Cretaceous. Am. J. Sci. 301, 112–149.

Jones, C.E., Jenkyns, H.C., Hesselbo, S.P., 1994a. Strontium isotopes in Early Jurassic seawater. Geochim. Cosmochim. Acta 58, 1285–1301.

Jones, C.E., Jenkyns, H.C., Coe, A.L., Hesselbo, S.P., 1994b. Strontium isotopes in Jurassic and Cretaceous seawater. Geochim. Cosmochim. Acta 58, 3061–3074.

Kuleva, G.V., Yanochkina, Z.A., Bukina, T.F., 1996. Paleoecosystem of *Dorsoplanites panderi* phase in the Volga Shale-generating basin. Stratigr. Geol. Correl. 4, 238–245.

Küspert, W., 1982. Environmental changes during oil shale deposition as deduced from stable isotope ratios. In: Einsele, G., Seilacher, A. (Eds.), Cyclic and Event Stratification. Springer, Berlin, pp. 482–501.

Lecuyer, C., Allemand, P., 1999. Modelling of the oxygen isotope evolution of seawater: Implications for the climate interpretation of the $\delta^{18}O$ of marine sediments. Geochim. Cosmochim. Acta 63, 351–361.

Marshall, J.D., 1992. Climatic and oceanographic isotopic signals from the carbonate rock record and their preservation. Geol. Mag. 129, 143–160.

McArthur, J.M., 1994. Recent trends in strontium isotope stratigraphy. Terra Nova 6, 331–358.

Mesook, A., Grant-Mackie, J.A., 1995. Upper Jurassic stratigraphy, south Kawhia region, New Zealand. N.Z. J. Geol. Geophys. 38, 361–373.

Milliman, J.D., 1974. Marine Carbonates. Springer, Berlin.

Monger, J.W.H., 1998. The Candian Cordillera: Geology and tectonic evolution. In: Smith, P.L. (Ed.), Field Guide for the Fifth International Symposium on the Jurassic System. The Geological Survey of Canada, Vancouver, pp. 5–28.

Morrison, J.O., Brand, U., 1986. Geochemistry of recent marine invertebrates. Geosci. Can. 13, 237–254.

Mutterlose, J., Kessels, K., 2000. Early Cretaceous nannofossil variation from the Norwegian North Sea and Antarctic Shelf reflect latitudinal climate belts. Palaeogeogr. Palaeoclimatol. Palaeoecol. 156, 173–187.

Padden, M., Weissert, H., Funk, H., Schneider, S., Gansner, C., 2002. Late Jurassic lithological evolution and carbon-isotope stratigraphy of the western Tethys. Eclogae Geol. Helv. 95, 333–346.

Pálfy, J., Smith, P.L., Mortensen, J.K., 2000. A U–Pb and $^{40}Ar/^{39}Ar$ time scale for the Jurassic. Can. J. Earth Sci. 37, 923–944.

Palmer, M.R., Elderfield, H., 1985. Sr isotope composition of sea water over the past 75 Myr. Nature 314, 526–528.

Parrish, J.T., Curtis, R.L., 1982. Atmospheric circulation, upwelling, and organic-rich rocks in the Mesozoic and Cenozoic eras. Palaeogeogr. Palaeoclimatol. Palaeoecol. 40, 31–66.

Pirrie, D., Marshall, J.D., 1990. High-paleolatitude late Cretaceous paleotemperatures – new data from James Ross Island, Antarctica. Geology 18, 31–34.

Podlaha, O.G., 1995. Modellrechnungen auf der Basis hochauflösender Isotopenstratigraphie ($\delta^{13}C$, $\delta^{18}O$, $^{87}Sr/^{86}Sr$) des Jura und der Unteren Kreide (Bajoc-Barrême/Apt). Ph.D. Thesis, Ruhr-Universität Bochum.

Podlaha, O.G., Mutterlose, J., Veizer, J., 1998. Preservation of $\delta^{18}O$ and $\delta^{13}C$ in belemnite rostra from Jurassic/Early Cretaceous successions. Am. J. Sci. 298, 324–347.

Poulton, T.P., 1989. Upper Absaroka to Lower Zuni: The transition to the foreland basin. In: Ricketts, B.D. (Ed.), Western Canada Sedimentary Basin, A Case History. Canadian Society of Petroleum Geologists, Calgary, pp. 233–247.

Price, G.D., 1999. The evidence and implications of polar ice during the Mesozoic. Earth Sci. Rev. 48, 183–210.

Price, G.D., Gröcke, D.R., 2002. Strontium-isotope stratigraphy and oxygen- and carbon-isotope variation during the Middle Jurassic–Early Cretaceous of the Falkland Plateau, South Atlantic. Palaeogeogr. Palaeoclimatol. Palaeoecol. 183, 209–222.

Price, G.D., Ruffell, A.H., Jones, C.E., Kalin, R.M., Mutterlose, J., 2000. Isotopic evidence for temperature variation during the early Cretaceous (late Ryazanian–mid Hauterivian). J. Geol. Soc. Lond. 157, 335–343.

Price, G.D., Sellwood, B.W., 1994. Palaeotemperatures indicated by Upper Jurassic (Kimmeridgian–Tithonian) fossils from Mallorca determined by oxygen isotope composition. Palaeogeogr. Palaeoclimatol. Palaeoecol. 110, 1–10.

Price, G.D., Sellwood, B.W., 1997. 'Warm' palaeotemperatures from high late Jurassic palaeolatitudes (Falkland Plateau): Ecological, environmental or diagenetic controls? Palaeogeogr. Palaeoclimatol. Palaeoecol. 129, 315–327.

Price, G.D., Sellwood, B.W., Valdes, P.J., 1995. Sedimentological evaluation of General Circulation Model simulations for the greenhouse Earth: Cretaceous and Jurassic case studies. Sediment. Geol. 100, 159–180.

Price, G.D., Valdes, P.J., Sellwood, B.W., 1998. A comparison of GCM simulated Cretaceous 'Greenhouse' and 'Icehouse' climates: Implications for the sedimentary record. Palaeogeogr. Palaeoclimatol. Palaeoecol. 142, 123–138.

Riboulleau, A., Baudin, F., Daux, V., Hantzpergue, P., Renard, M., Zakharov, V., 1998. Évolution de la paléotempérature de eaux de la plate-forme russe au cours du Jurassique supérieur. C. R. Acad. Sci. Ser. II 326, 239–246.

Robinson, S.A., Andrews, J.E., Hesselbo, S.P., Radley, J.D., Dennis, P.F., Harding, I.C., Allen, P., 2002. Atmospheric pCO_2 and depositional environment from stable-isotope geochemistry of calcrete nodules (Barremian, Lower Cretaceous, Wealden Beds, England). J. Geol. Soc. Lond. 159, 215–224.

Ruffell, A.H., Rawson, P.F., 1994. Paleoclimate control on sequence stratigraphic patterns in the late Jurassic to mid-Cretaceous, with a case-study from eastern England. Palaeogeogr. Palaeoclimatol. Palaeoecol. 110, 43–54.

Ruffell, A., McKinley, J.M., Worden, R.H., 2002. Comparison of clay mineral stratigraphy to other proxy palaeoclimate indicators in the Mesozoic of NW Europe. In: Gröcke, D.R., Kucera, M. (Eds.), Understanding climate change: proxies, chronology and ocean-atmosphere interactions. Phil. Trans. R. Soc. Lond. A 360, 675–693.

Sahagian, D., Pinous, O., Olferiev, A., Zakharov, V., 1996. Eustatic curve for the Middle Jurassic–Cretaceous based on Russian platform and Siberian stratigraphy: Zonal resolution. Bull. Am. Assoc. Pet. Geol. 80, 1433–1458.

Saks, V.N., Shulgina, N.I., 1973. Correlation of the Jurassic–Cretaceous boundary beds in the Boreal Realm. In: Casey, R., Rawson, P.F. (Eds.), The Boreal Lower Cretaceous. Geol. J. 5, 387–393.

Sazonova, I.G., Sazanov, N.T., 1967. Paleogeography of Russian Platform in Jurassic and Cretaceous (in Russian). Trudy Vsesojuz. Nauch.-issled. Geol.-razv. Neft. Inst. 62, 1–126.

Sellwood, B.W., Valdes, P.J., Price, G.D., 2000. Geological

evaluation of multiple general circulation model simulations of Late Jurassic palaeoclimate. Palaeogeogr. Palaeoclimatol. Palaeoecol. 156, 147–160.

Shackleton, N.J., Kennett, J.P., 1975. Paleotemperature history of the Cenozoic and the initiation of Antarctic glaciation: Oxygen and carbon isotope analyses in DSDP Sites 277, 279 and 281. In: Kennett, J.P., Houtz, R.E., et al. (Eds.), Initial Reports of the Deep Sea Drilling Project 29, pp. 743–756.

Sheridan, R.E., 1997. Pulsation tectonics as a control on the dispersal and assembly of supercontinents. J. Geodyn. 23, 173–196.

Shulgina, N.I., 1985. Boreal basins on the Jurassic/Cretaceous border (in Russian). Vniiokeangeologia, Trudy 193, Nedra Press, Leningrad.

Shulgina, N.I., 1996. Biostratigraphic chart for the Lower Cretaceous of the central and eastern European (Russian) platform. Mitt. Geol. Paläontol. Inst. Univ. Hamburg 77, 89–93.

Smith, A.G., Smith, D.G., Funnell, B.M., 1994. Atlas of Mesozoic and Cenozoic Coastlines. Cambridge University Press, Cambridge.

Smith, E., Vazquez, J., Tran, A., Sumagaysay, R., 1996. Satellite-derived Sea Surface Temperature Data. NOAA/NASA Pathfinder Program (http://www.agu.org/eos_elec/95274e.html).

Stevens, G.R., 1992. The New Zealand Late Jurassic: Age assessments based on ammonite faunas.. Geol. Soc. N.Z. Miscell. Publ. 63A, 148.

Stevens, G.R., Clayton, R.N., 1971. Oxygen isotope studies on Jurassic and Cretaceous belemnites from New Zealand and their biogeographic significance. N.Z. J. Geol. Geophys. 14, 829–897.

Stoll, H.M., Schrag, D.P., 1996. Evidence of glacial control of rapid sea level changes in the early Cretaceous. Science 272, 1771–1774.

Teys, R.V., Naydin, D.P., Saks, V.N., 1968. Determination of Late Jurassic and Early Cretaceous paleotemperatures by the oxygen isotopic composition of belemnite rostra (in Russian). Trudy Instituta Geologii I Geofiziki (Novosibirsk) 48, 51–71.

Weissert, H., Channell, J.E.T., 1989. Tethyan carbonate carbon isotope stratigraphy across the Jurassic–Cretaceous boundary: An indicator of decelerated carbon cycling. Paleoceanography 4, 483–494.

Weissert, H., Lini, A., 1991. Ice Age interludes during the time of Cretaceous greenhouse climate? In: Mueller, D.W., McKenzie, J.A., Weissert, H. (Eds.), Controversies in Modern Geology. Academic Press, London, pp. 173–191.

Weissert, H., Mohr, H., 1996. Late Jurassic climate and its impact on carbon cycling. Palaeogeogr. Palaeoclimatol. Palaeoecol. 122, 27–43.

Weissert, H., Lini, A., Föllmi, K.B., Kuhn, O., 1998. Correlation of Early Cretaceous carbon isotope stratigraphy and platform drowning events: A possible link? Palaeogeogr. Palaeoclimatol. Palaeoecol. 137, 189–203.

Zeebe, R.E., 2002. CO_2 in seawater: equilibrium, kinetics, isotopes. Elsevier, Amsterdam.

Ziegler, P.A., 1990. Geological Atlas of Western and Central Europe, 2nd ed. Shell, The Hague.